Cloaked electromagnetic, acoustic, and quantum amplifiers via transformation optics

Allan Greenleaf[a], Yaroslav Kurylev[b], Matti Lassas[c], Ulf Leonhardt[d], and Gunther Uhlmann[e,f,1]

[a]Department of Mathematics, University of Rochester, Rochester, NY 14627; [b]Department of Mathematics, University College London, London WC1E 6BT, United Kingdom; [c]Department of Mathematics and Statistics, University of Helsinki, 00014, Helsinki, Finland; [d]School of Physics and Astronomy, University of St. Andrews, St. Andrews, KY16 9SS, Scotland, United Kingdom; [e]Department of Mathematics, University of Washington, Seattle, WA 98195; and [f]Department of Mathematics, University of California, Irvine, CA 92697

Edited by George C. Papanicolaou, Stanford University, Stanford, CA, and approved April 5, 2012 (received for review October 23, 2011)

The advent of transformation optics and metamaterials has made possible devices producing extreme effects on wave propagation. Here we describe a class of invisible reservoirs and amplifiers for waves, which we refer to as *Schrödinger hats*. The unifying mathematical principle on which these are based admits such devices for any time harmonic waves modeled by either the Helmholtz or Schrödinger equation, e.g., polarized waves in electromagnetism, acoustical waves and matter waves in quantum mechanics. Schrödinger hats occupy one part of a parameter-space continuum of wave-manipulating structures which also contains standard transformation optics based cloaks, resonant cloaks and cloaked sensors. Possible applications include near-field quantum microscopy.

field amplifiers | invisibility cloaking | improved cloaking | imaging

Transformation optics and metamaterials have made possible designs and devices producing effects on wave propagation not seen in nature, including invisibility cloaks for electrostatics (1, 2), electromagnetism (EM) (3–5), acoustics (6–8) and quantum mechanics (QM) (9); devices inspired by general relativity (10, 11) and non-Euclidian geometry (12); field rotators (13); EM wormholes (14); and illusion optics (15), among many others. See (16) for an overview. At nonzero frequencies, ideal (i.e., perfect) cloaking produces a decoupling between the parts of the wave in the cloaked region and its exterior, and one has both cloaking (the undetectability of the object within the cloak) and shielding (the inability of the wave to penetrate into the cloaked region) (17). In more realistic approximate cloaking, there is generically only a weak coupling between the regions; however, if the frequency (for acoustic or EM cloaks) or energy (for QM cloaks) is an eigenvalue for the interior region, then there exist resonant (or trapped) states which simultaneously destroy both cloaking and shielding (18, 19, 20). Near such a resonance, it is possible to design the cloak parameters so that the flow of the wave from the exterior into the cloak and vice versa are precisely balanced. This restores and even improves cloaking, while allowing a moderate penetration of the cloaked region by the incident wave (21), leading to the possibility of transformation optics-based cloaked sensors. A different approach previously led to sensors in plasmonic cloaking (22).

Purpose of Paper

We show here that it is possible to go beyond the limited coupling allowed by cloaked sensors and give designs, based on an overarching mathematical principle, for devices which we call *Schrödinger hats*, acting as invisible reservoirs and amplifiers for waves and particles. Schrödinger hats (SH) exist for any wave phenomenon modeled by either the Helmholtz or Schrödinger equation. They are specified by either a mass density/bulk modulus pair (for Helmholtz) or a potential (for Schrödinger), and come in families which increasingly exhibit their characteristic properties as the parameters ϵ and ρ go to zero.

A SH seizes a large fraction of a time harmonic incident wave, holding and amplifying it while contributing only a negligible amount to scattering; see Fig. 1. In quantum mechanics, despite the localization of the resulting matter waves, SH are nevertheless consistent with the Heisenberg uncertainty principle. We briefly describe possible implementations of Schrödinger hats. Highly oscillatory potentials are needed for QM Schrödinger hats, and we propose several realizations; one possible application is for a near-field scanning quantum microscope. The less demanding acoustic and EM hats offer similar effects, but existing metamaterials (23–26) should make these Schrödinger hats more immediately realizable, allowing physical verification and further exploration of the concept.

Outline of the Construction

Schrödinger hats are formed from approximate cloaks surrounding layers of barriers and wells. These can be implemented as follows, starting from the ideal 3D spherical transformation optics EM invisibility cloak (4). One subjects homogeneous, isotropic permittivity ε_0 and permeability μ_0 to the 'blowing up a point' coordinate transformation (1, 2, 4), $\mathbf{x} := F(\mathbf{y}) = (1+|\mathbf{y}|/2)\mathbf{y}/|\mathbf{y}|$, for $0 < |\mathbf{y}| \le 2$,

$$\mathbf{x} = F(\mathbf{y}) = \left(1 + \frac{|\mathbf{y}|}{2}\right)\frac{\mathbf{y}}{|\mathbf{y}|}, \quad \text{for } 0 < |\mathbf{y}| \le 2, \qquad [1]$$

used to cloak the ball B_1 of radius 1 centered at origin. This works equally well in acoustics (7, 8, 27), and we now use the terminology from that setting. The resulting cloak consists of a spherically symmetric, anisotropic mass density $\mathbb{M}$ and bulk modulus λ , both singular as $r := |\mathbf{x}| \to 1$. For any $0 < \rho < 1$, the ideal cloak can then be approximated by replacing $\mathbb{M}$ by the identity matrix $\mathbb{I}$ and the bulk modulus by 1 in the shell $B_R - B_1 = \{\mathbf{x} \in \mathbb{R}^3 : \ R > |\mathbf{x}| \ge 1\}$, where $R = 1 + \rho/2$. This results in a nonsingular (but still anisotropic) mass density $\mathbb{M}_\rho$ and bulk modulus λ_ρ, which converge to the ideal cloak parameters as $\rho \to 0$. Via homogenization theory, $\mathbb{M}_\rho$ is (roughly speaking) approximable by *isotropic* mass densities $m_{\rho,\varepsilon}$, consisting of shells of small thickness having alternating large and small densities, yielding a family of approximate cloaks (19), modeled by the Helmholtz equation $(\nabla \cdot m_{\rho,\varepsilon} \nabla + \lambda_\rho \omega^2)u = 0$. One then obtains an approximate QM cloak by applying the Liouville-gauge transformation, substituting $\psi(\mathbf{x}) = m_{\rho,\varepsilon}^{-1/2}(\mathbf{x})u(\mathbf{x})$. Indeed, when u solves the Helmholtz equation, ψ satisfies the time independent Schrödinger equation, $(-\nabla^2 + V_c - E)\psi = 0$, where $E = \omega^2$ is the energy and $V_c = (1 - m_{\rho,\varepsilon}\lambda_\rho^{-1})E + m_\varepsilon^{1/2}\nabla^2(m_{\rho,\varepsilon}^{-1/2})$ is the cloaking potential for the energy level E.

Author contributions: A.G., Y.K., M.L., U.L., and G.U. have equally performed research and wrote the paper. (Authors are listed in alphabetical order.)

The authors declare no conflict of interest.

This article is a PNAS Direct Submission.

Freely available online through the PNAS open access option.

[1]To whom correspondence should be addressed. E-mail: gunther@math.washington.edu.

This article contains supporting information online at www.pnas.org/lookup/suppl/doi:10.1073/pnas.1116864109/-/DCSupplemental.

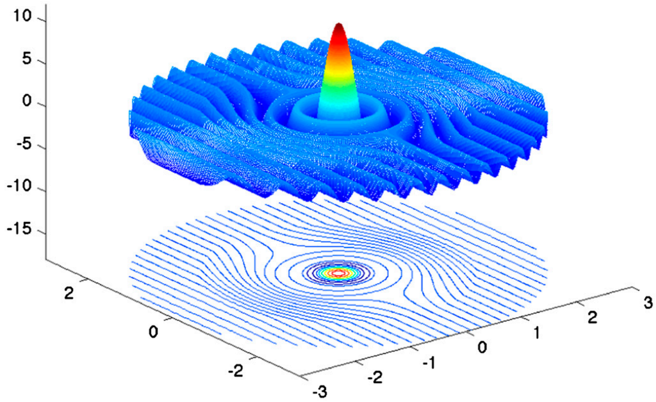

Fig. 1. A quasmon inside a Schrödinger hat. The real part of the effective wave function $\psi^{\mathrm{sh}}_{\mathrm{eff}}(x, y, z)$ at the plane $z = 0$ when a plane wave is incident to a SH potential. By varying the design parameters, the concentration of the wave inside the cloaked region can be made arbitrarily strong and the scattered field arbitrarily small. The matter wave is spatially localized, but conforms to the uncertainty principle, with the large gradient, visible as the steep slope of the central peak, concentrating the momentum in a spherical shell in p-space. For definition of $\psi^{\mathrm{sh}}_{\mathrm{eff}}$ and a video of time harmonic wave, see (*SI Text* and Movie S1). For comparison with non-Schrödinger hat cloaks, see Fig. 2 and Fig. S1. The wave function with another incident wave is shown in Fig. S2.

For acoustic or EM cloaks constructed using positive index materials, resonances can allow large amounts of energy to be stored inside the 'cloaked' region, but at the price of destroying the cloaking effect (18, 19), particularly strongly in the near field. However, here we show that inserting materials with negative bulk modulus or permittivity within the cloaked region allows for the cloaked storage of arbitrarily large amounts of energy. A similar effect was described in two-dimensional superlenses, where nonradiating (i.e., cloaked) high-energy concentrations can appear due to anomalous resonance (28, 29); see discussion in (*SI Text*). For brevity, we describe Schrödinger hats primarily in the context of QM cloaking, where the analogous effect is concentration of probability density. When the cloaking potential is augmented by a layered internal potential consisting of N shells, alternating positive barriers and negative wells with appropriately chosen parameters, the probability of the particle being inside the cloaked region can be made as close to 1 as desired. For simplicity, we restrict ourselves to $N = 2$ for some of the discussion and simulations, but larger values of N allow for central excitations, or *quasmons*, with arbitrarily many sign crossings. More precisely, insert into B_1 a piecewise constant potential $Q(\mathbf{x})$, consisting of two layers with values τ_1 in B_{s_1}, τ_2 in $B_{s_2} - B_{s_1}$, and zero elsewhere. For suitable parameters ρ, ϵ, s_j and τ_j of the potential Q, we obtain (*SI Text*) a Schrödinger hat potential, $V_{\mathrm{SH}} = V_c + Q$. Matter waves with energy E that are incident on the SH are modeled by Schrödinger's equation, $(-\nabla^2 + V_{\mathrm{SH}} - E)\psi = 0$.

The key feature of V_{SH} is that the resulting matter waves can be made to concentrate inside the cloaked region as much as desired, while nevertheless maintaining the cloaking effect, quantified as follows. Assume that we have two balls of radius $L > 2$, B_L^{em} and B_L^{sh}, containing empty space and a Schrödinger hat, resp. Let $B_1^{\cdot}, B_2^{\cdot}$ denote the balls of radii 1 and 2, resp., centered at 0, for $\cdot$:= em or sh, and assume that matter waves ψ^{em} and ψ^{sh} on $B_L^{\mathrm{em}}, B_L^{\mathrm{sh}}$, resp., have the same boundary values on the sphere of radius L, corresponding to identical incident waves. Define the *strength* of the Schrödinger hat to be the dimensionless ratio

$$\mathfrak{S} = \frac{1}{\mathrm{vol}(B_1)|\psi^{\mathrm{em}}(0)|^2} \int_{B_1^{\mathrm{SH}}} |\psi^{\mathrm{sh}}(\mathbf{x})|^2 d\mathbf{x}, \qquad [2]$$

where ψ^{em} and ψ^{sh} are solutions which coincide in $|\mathbf{x}| > 2$. We show that, by appropriate choice of the design parameters, $\mathfrak{S}$ may be made to take any prescribed positive value. For large values of $\mathfrak{S}$, the probability density of ψ^{sh} is almost completely concentrated in the cloaked region.

Properties. Schrödinger hats have some remarkable effects on wave propagation.

- They act as reservoirs, capturing, amplifying and storing energy from incident time harmonic acoustic or EM waves, or probability density from incident matter waves in QM. We remark that potentials which, for *some* incident wave, produce a scattered wave which is *exactly* zero outside a bounded set, are said to have a transmission eigenvalue (30). In contrast, the scattered wave caused by a Schrödinger hat potential is *approximately* zero for *all* incident fields.
- The amplification and concentration of a matter wave in the cloaked region can be used to create probabilistic illusions. For any $L > 2$, consider (nonnormalized) wave functions ψ^{em} and ψ^{sh} on B_L, for empty space and a SH in B_2, resp., which coincide in the shell $B_L - B_2$. Then for any region $\mathscr{R} \subset B_L - B_2$ the conditional probability that the particle is observed to be in $\mathscr{R}$, given that it is observed in $B_L - B_2$, is the same for ψ^{em} and ψ^{sh}. However, by choosing the parameters of the SH appropriately, the probability that the particle ψ^{sh} is in the cloaked region B_1 can be made as close to 1 as wished. The particle ψ^{sh} is like a trapped ghost of the particle ψ^{em} in that it is located in the exterior of the SH structure with far lower probability than ψ^{em} is, but when ψ^{sh} is observed in $B_L - B_2$, all of its time harmonic measurements coincide with those of ψ^{em} (see Fig. S3).
- The highly concentrated part of the wave function inside the cloaked region of a QM Schrödinger hat is, as mentioned above, a localized excitation which we refer to as a *quasmon*. The strong concentration of the wave function in B_1, without change to the wave function outside the ball B_2 where the SH potential is supported, is nevertheless consistent with the uncertainty principle: although the particle is spatially localized within B_1, the variation of its momentum is large, due to the large gradient of ψ^{sh} on a spherical shell about the central peak; cf. Figs. 1 and 2 (red), and Fig. S3.
- A quasmon excited within a QM Schrödinger hat has a well-defined electric charge and variance of momentum, depending on the parameters of the hat. The Schrödinger hat produces vanishingly small changes in the matter wave outside of the cloak, while simultaneously making the particle concentrate inside the cloaked region. Thus, if the matter wave is charged, it may couple via Coulomb interaction with other particles or measurement devices external to the cloak. When a time harmonic incident field ψ^{in} is scattered by the SH, the field is only perturbed negligibly outside of the support of the hat potential, V_{SH}; there is essentially no scattering. However, the Schrödinger hat concentrates the charge inside the cloaked region, proportional to $|\psi^{\mathrm{in}}(0)|^2$, the square of the modulus of the value which the incident field would have had at the center of B_L in the absence of the SH. Due to the long range nature of the Coulomb potential, this charge causes an electric field which can be measured even far away from the SH. If the result is zero, this indicates that $\psi^{\mathrm{in}}(0) = 0$; without disturbing the field, one determines whether the incident field vanishes at 0 (see *SI Text*). Generically, the nodal set for a complex-valued wave function in 3D is a curve; however, if an electric potential is real and there is no magnetic field, then the real and imaginary parts of the wave can be linearly dependent and the nodal set is a surface. In either case, a measuring device within a Schrödinger hat can act as a non–interacting sensor, detecting, for an ensemble of quantum systems, the nodal set on which the incident matter wave vanishes, allowing for possible

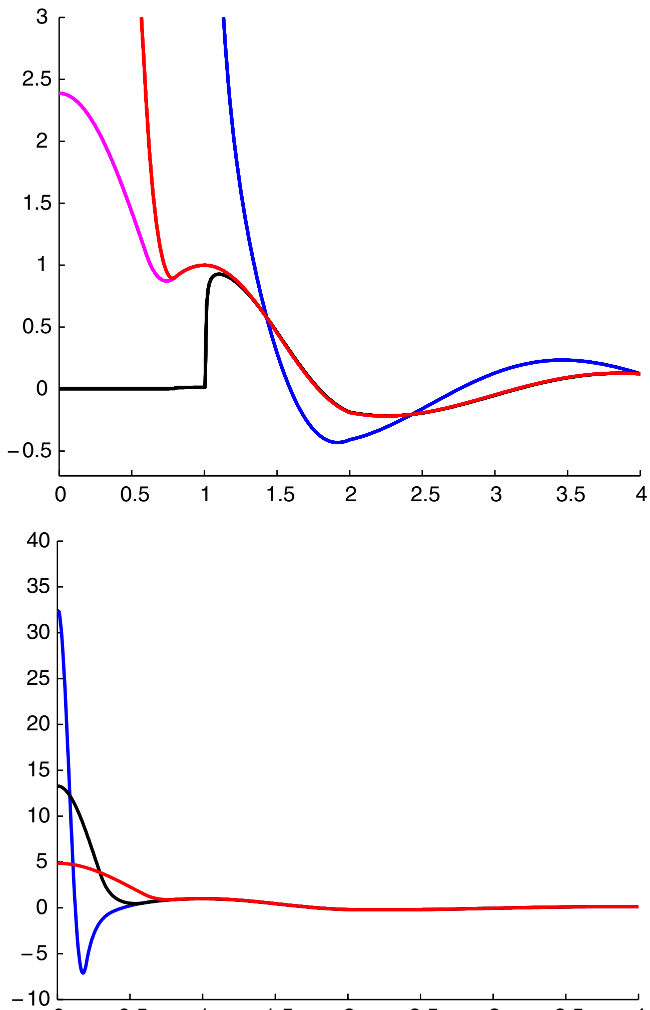

Fig. 2. The cloak–resonance–sensor–Schrödinger hat continuum. Scattering by potentials with different parameters, demonstrating four modes: cloak, resonance, sensor and Schrödinger hat. Graphs show the real parts of $\tilde{u}$ (defined in Thm. 1) for $0 \le r \le 4$; note different vertical scales. *Upper*: Cloak (black) allows little penetration of incident wave into cloaked region, B_1. Resonant curve (blue) shows blowup (to off-chart values, see Fig. S1) within B_1, and large near-field deviation from incident wave, indicating failure of cloaking. Sensor (purple) combines cloaking effect with moderate penetration into B_1. Schrödinger hat (red) obtains large value within B_1, allowing for very sensitive cloaked measurement of incident waves. Note that the cloak, sensor and SH solutions are essentially identical with the incident wave outside of the cloaked region, while the resonant solution diverges, destroying cloaking (18, 19). *Lower*: Continuous parameter variation from sensor to Schrödinger hat modes. Height of central excitation (quasmon) can be made arbitrarily large, and width of peak made arbitrarily small. For parameters used, see (*SI Text*).

near-field scanning quantum microscopy, analogous to cloaked acoustic and EM sensors (21, 22) and near-field optical microscopes (31).

Details of the Construction. The two main ingredients of Schrödinger hats are approximate cloaks and barrier/well layers. We start by recalling some facts concerning nonsingular approximations to ideal 3D spherical cloaks (18, 19, 20, 32, 33). For $0 \le \rho < 2$, set $R = 1 + \frac{1}{2}\rho$, so that $R \to 1$ as $\rho \to 0$; as above, our asymptotics will be in terms of ρ. Let $B_R = \{|\mathbf{x}| < R\}$, $\bar{B}_R = \{|\mathbf{x}| \le R\}$ and $S_R = \{|\mathbf{x}| = R\}$ be the open ball, closed ball and sphere centered at the origin 0 and of radius R, resp. Introduce the coordinate transformation $F_\rho : B_L - B_\rho \to B_L - B_R$,

$$\mathbf{x} := F_\rho(\mathbf{y}) = \begin{cases} \mathbf{y}, & \text{for } 2 < |\mathbf{y}| < L, \\ \left(1 + \frac{|\mathbf{y}|}{2}\right) \frac{\mathbf{y}}{|\mathbf{y}|}, & \text{for } \rho < |\mathbf{y}| \le 2. \end{cases} \qquad \textbf{[3]}$$

For $\rho = 0$ (that is, $R = 1$), this is the singular transformation **[1]**, leading to the ideal cloak, while for $\rho > 0$ (that is, $R > 1$), F_ρ is nonsingular and leads to a class of approximate cloaks (18, 19, 20, 32, 34). If we set $\mathbb{I} = (\delta_{jk})$ denotes the identity matrix, then, for $\rho = 0$, this pushes forward into an anisotropic singular mass tensor, $(\mathbb{M}_0)_{jk}(\mathbf{x})$, on $B_L - B_1$, defined in terms of its inverse,

$$\begin{aligned}(\mathbb{M}_0^{-1})^{jk}(\mathbf{x}) &= ((F_0)_*\mathbb{I})^{jk}(\mathbf{y}) \\ &:= \frac{1}{\det\left[\frac{\partial F_0}{\partial x}(\mathbf{x})\right]} \sum_{p,q=1}^{3} \frac{\partial (F_0)^j}{\partial x^p}(\mathbf{x}) \frac{\partial (F_0)^k}{\partial x^q}(\mathbf{x}) \delta^{pq}(\mathbf{x}) \Big|_{\mathbf{x}=F_0^{-1}(\mathbf{y})}.\end{aligned}$$

$\mathbb{M}_0(\mathbf{x})$ is the matrix-valued function on $B_2 - B_1$ with elements

$$(\mathbb{M}_0)_{jk}(\mathbf{x}) = \frac{1}{2}(\delta_{jk} - P_{jk}(\mathbf{x})) + \frac{1}{2}(|\mathbf{x}| - 1)^{-2}|\mathbf{x}|^2 P_{jk}(\mathbf{x}),$$

where the matrix $P(\mathbf{x})$, having elements $P_{jk}(\mathbf{x}) = |\mathbf{x}|^{-2} x_j x_k$, is the projection to the radial direction. On the other hand, when $\rho > 0$, we obtain an anisotropic but nonsingular mass tensor, $\mathbb{M}_\rho(\mathbf{x})$, on $B_L - B_R$, given by

$$\begin{aligned}(\mathbb{M}_\rho^{-1})^{jk}(\mathbf{x}) &= ((F_\rho)_*\mathbb{I})^{jk}(\mathbf{y}) \\ &:= \frac{1}{\det\left[\frac{\partial F_\rho}{\partial x}(\mathbf{x})\right]} \sum_{p,q=1}^{3} \frac{\partial (F_\rho)^j}{\partial x^p}(\mathbf{x}) \frac{\partial (F_\rho)^k}{\partial x^q}(\mathbf{x}) \delta^{pq}(\mathbf{x}) \Big|_{\mathbf{x}=F_\rho^{-1}(\mathbf{y})},\end{aligned} \qquad \textbf{[4]}$$

and $\mathbb{M}_\rho(\mathbf{x}) = \mathbb{I}$ on $B_R \cup (B_L - B_2)$. For each $\rho > 0$, the eigenvalues of $\mathbb{M}_\rho$ are bounded from above and below; however, one of them tend to ∞ as $\rho \to 0$. Fixing an $R_0 < 1$, we also define a scalar bulk modulus function $\lambda_\rho(\mathbf{x})$ on B_L,

$$\lambda_\rho(\mathbf{x}) = \begin{cases} \eta(\mathbf{x}), & \mathbf{x} \in B_{R_0}, \\ \frac{1}{8}|\mathbf{x}|^2(|\mathbf{x}| - 1)^{-2}, & \mathbf{x} \in B_2 - B_R, \\ 1, & \mathbf{x} \in (B_R - B_{R_0}) \cup (B_L - B_2) \end{cases} \qquad \textbf{[5]}$$

where η is a layered combination of barriers and wells,

$$\eta(\mathbf{x}) = \eta(\mathbf{x}; \tau) = \sum_{j=1}^{N} \frac{1}{\tau_j} \chi_{(s_{j-1}, s_j)}(|\mathbf{x}|). \qquad \textbf{[6]}$$

Here $\tau = (\tau_1, \tau_2, \ldots, \tau_N)$, $\tau_j \in \mathbb{R}$ are parameters which one can vary, $0 = s_0 < s_j < s_N = R_0$ are some fixed numbers, and $\chi_{(s_{j-1}, s_j)}(r) = 1$ on the interval (s_{j-1}, s_j) and vanishes elsewhere. Thus, we have a homogeneous ball B_{s_0} coated with concentric homogeneous shells, sometimes writing $\lambda_\rho(\mathbf{x}) = \lambda_\rho(\mathbf{x}; \tau)$. While in acoustics λ_ρ denotes the bulk modulus, in quantum mechanics later, λ_ρ^{-1} will give rise to the potential.

Next, consider in the domain B_L the solutions of the boundary value problem,

$$(-\nabla \cdot \mathbb{M}_\rho^{-1} \nabla - \omega^2 \lambda_\rho^{-1}) u_\rho = 0 \quad \text{in } B_L, \qquad u_\rho|_{S_L} = h. \qquad \textbf{[7]}$$

Since the matrix $\mathbb{M}_\rho$ is nonsingular everywhere, across the internal interface S_R we have the standard transmission conditions,

$$u_\rho|_{S_{R^+}} = u_\rho|_{S_{R^-}}, \qquad \mathbf{e_r} \cdot (\mathbb{M}_\rho^{-1} \nabla u_\rho)|_{S_{R^+}} = \mathbf{e_r} \cdot (\mathbb{M}_\rho^{-1} \nabla u_\rho)|_{S_{R^-}}, \qquad \textbf{[8]}$$

where $\mathbf{e_r}$ is the radial unit vector and the $\pm$ indicates the the boundary value on S_R as $r \to R^\pm$. In the physical space / virtual space paradigm of transformation optics, here the physical space is B_L, and the virtual space is a disjoint union, $(B_L - B_\rho) \cup B_R$. On the ball B_L in physical space, one has

$$u_\rho(\mathbf{x}) = \begin{cases} v_\rho^+(F_\rho^{-1}(\mathbf{x})), & \mathbf{x} \in B_L - B_R, \\ v_\rho^-(\mathbf{x}), & \mathbf{x} \in B_R, \end{cases} \quad [9]$$

where $v_\rho^\pm$, on the virtual space, is the solution of

$$(-\nabla^2 - \omega^2)v_\rho^+(\mathbf{y}) = 0, \qquad \mathbf{y} \in B_L - B_\rho, \qquad v_\rho^+|_{S_L} = h,$$

and

$$(-\nabla^2 - \omega^2\lambda_\rho^{-1})v_\rho^-(\mathbf{y}) = 0, \qquad \mathbf{y} \in B_R. \quad [10]$$

With respect to spherical coordinates (r, θ, φ), the transmission conditions **[8]** become

$$\begin{aligned} v_\rho^+(\rho, \theta, \phi) &= v_\rho^-(R, \theta, \phi), \\ \rho^2 \partial_r v_\rho^+(\rho, \theta, \phi) &= R^2 \partial_r v_\rho^-(R, \theta, \phi). \end{aligned} \quad [11]$$

Since $\mathbb{M}_\rho, \lambda_\rho$ are spherically symmetric, cf. **[4, 5]**, we can separate variables in **[7]**, writing u_ρ as

$$u_\rho(r, \theta, \phi) = \sum_{n=0}^{\infty} \sum_{m=-n}^{n} u_\rho^{nm}(r) Y_n^m(\theta, \phi), \quad [12]$$

where Y_n^m are the standard spherical harmonics, giving rise to a family of boundary value problems for the u_ρ^{nm}. The most important term, which we now analyze, is the lowest harmonic (the s-mode), $u_\rho^{0,0}$, i.e., the radial component of u_ρ.

The Lowest Harmonic. Consider the asymptotics as $\rho \to 0$ of the Dirichlet problem,

$$(-\nabla \cdot \mathbb{M}_\rho^{-1}\nabla - \omega^2\lambda_\rho^{-1})u_\rho = 0 \quad \text{in } B_L, \qquad u_\rho|_{S_L} = h(\mathbf{x}). \quad [13]$$

We have shown (19) that for a specific value of the parameter $\tau \in \mathbb{R}^N$, denoted $\tau = \tau^{\text{res}}(\rho)$, such that the equation **13** has a nonzero radial solution with $h = 0$, there is an interior resonance, destroying cloaking. The field u_ρ grows larger inside the cloaked region as $\rho \to 0$, and this resonance is detectable, both by (near-field) boundary measurements outside of the cloak and (far-field) scattering data.

On the other hand, for another value of τ, denoted $\tau = \tau^{\text{sh}}(\rho)$, the cloak acts as an approximate cloak and inside the cloaked region the solution is proportional to the value which the field in the empty space would have at the origin. This corresponds to the equation **13** having a radial solution u_ρ which satisfies $\partial_r u_\rho(L) = \omega j_0'(\omega L)$ and $u_\rho(L) = j_0(\omega L)$, or equivalently, $u_\rho(\mathbf{x}) = j_0(\omega|\mathbf{x}|)$ for $\mathbf{x} \in B_L - B_R$. Due to the transmission condition **[8]** we see that the values $\tau^{\text{res}}(\rho)$ and $\tau^{\text{sh}}(\rho)$ are close, with $\lim_{\rho\to 0}\tau^{\text{sh}}(\rho) - \tau^{\text{res}}(\rho) = 0$.

We now explain how to find $\tau = \tau^{\text{sh}}(\rho)$; note that $\tau^{\text{sh}}(\rho)$ depends on ω, $\rho > 0$, and $0 < R_0 < 1$, but these parameters are omitted in the notation below. For simplicity, we work with $N = 2$. Consider the ODE corresponding to the radial solutions $u(r)$ of the equation **13**, i.e.,

$$-\frac{1}{r^2}\frac{d}{dr}\left(r^2\sigma_\rho(r)\frac{d}{dr}u(r)\right) - \omega^2\lambda_\rho^{-1}(r)u(r) = 0, \quad [14]$$

and pose the Cauchy data (i.e., initial data) at $r = L$, $u(L) = j_0(L\omega)$, $\partial_r u(L) = \omega j_0'(L\omega)$. Here, $\sigma_\rho(r)$ is the rr-component of the matrix $\mathbb{M}_\rho^{-1}$, that is, $\sigma_\rho(r) = 2(r-1)^2$, for $R < r < 2$ and $\sigma_\rho(r) = 1$ elsewhere. We solve the initial value problem for **[14]** for r on the interval $[R_0, L]$, and find the Cauchy data $(u(R_0), u'(R_0))$ at $r = R_0$, where $u' := \frac{du}{dr}$. Note that on the interval $[R_0, L]$, λ_ρ does not depend on τ. Consider the case when $s_1 = R_0/2$, $s_2 = R_0$ and $\tau = (\tau_1, \tau_2)$, where τ_1 and τ_2 are constructed as follows: First, choose τ_2 to be a negative number with a large absolute value. Then solve the initial value problem for **[14]** on $[s_1, R_0]$ with initial data $(u(R_0), u'(R_0))$ at $r = R_0$. In particular, this determines the Cauchy data $(u(s_1), u'(s_1))$ at $r = s_1$. Secondly, consider τ_1, τ_2, as well as ρ, R_0, to be parameters, and solve the initial value problem for **[14]** on interval $[0, s_1]$ with initial data $(u(s_1), u'(s_1))$ at $r = s_1$. Denote the solution by $u(r; \tau_1, \rho, R_0, \tau_2)$ and find the value $\frac{du}{dr}(r; \tau_1, \rho, R_0, \tau_2)|_{r=0}$. For ρ, R_0, and τ_2 given, find $\tau_1 > 0$ satisfying

$$\left.\frac{du}{dr}(r; \tau_1, \rho, R_0, \tau_2)\right|_{r=0} = 0. \quad [15]$$

We choose τ_1 to be a value for which **[15]** holds, and denote this solution by $\tau_1(\rho, R_0, \tau_2)$; choosing higher values for τ_1 leads to quasmons with larger numbers of sign changes. Set $\tau^{\text{sh}}(\rho) := (\tau_1(\rho, R_0, \tau_2), \tau_2)$. Summarizing the above computations, we have obtained a cloak at frequency ω, that is, for the energy $E_0 = \omega^2$, with radial solution $u(\mathbf{x})$ satisfing $u(\mathbf{x}) = j_0(\omega|\mathbf{x}|)$ for $|\mathbf{x}| \in [2, L]$. Moreover, when τ_2 is large, this solution $u_\rho(r)$ grows exponentially fast on the interval $[s_1, s_2]$, as r becomes smaller, while on the interval $[0, s_1]$ it satisfies $u'(0) = 0$, so that $u(r)$ defines a smooth spherically symmetric solution of **[13]**.

In the context of QM cloaks below, the construction above can be considered as follows: Inside the cloak there is a potential well of depth $-\tau_1$, enclosed by a potential barrier of height τ_2. The parameters τ_1 and τ_2 are chosen so that the solution is large inside the cloak due to the resonance there. The cloaked region is thus well–hidden even though the solution may be very large inside the cloaked region. In a fixed-energy scattering experiment, with high probability the potential captures the incoming particle, but due to the chosen parameters of the cloak, external measurements cannot detect this.

Using the implicit function theorem, one can show that for generic values of τ_2 and R_0, $\lim_{\rho\to 0}\tau_1(\rho, R_0, \tau_2) := \tau_1(R_0, \tau_2)$ exists. We note that the solution $u_\rho(r) := u(r; \tau_1(\rho, R_0, \tau_2), \rho, \tau_2)$ of **[14]** has limit $\lim_{\rho\to 0}u(r; \tau_1(\rho, R_0, \tau_2), \rho, \tau_2)) = c\Phi(r), \quad r < 1$, where $c \in \mathbb{C}$ and $\Phi(r) \not\equiv 0$ is an eigenfunction of the boundary value problem,

$$(\nabla^2 + \omega^2\lambda_0^{-1}(\mathbf{y}; \tau))\Phi(|\mathbf{y}|) = 0, \qquad \partial_r\Phi(|\mathbf{y}|)|_{r=1} = 0, \quad [16]$$

where $\tau = (\tau_1(R_0, \tau_2), \tau_2)$ and Φ is normalized so that $\|\Phi\|_{L^2(B_1)} = 1$. This finishes the analysis of the lowest harmonic; for the higher order harmonics, see (*SI Text*).

In summary: As $\rho \to 0$, in the region $B_L - B_2$ the solutions $u_\rho(\mathbf{x})$ converge to the solution u corresponding to the homogeneous virtual space boundary problem,

$$(-\nabla^2 - \omega^2)u = 0 \quad \text{in } B_L, \qquad u|_{S_L} = h(\mathbf{x}) \quad [17]$$

and, in the cloaked region B_1, to the solution in empty space,

$$\lim_{\rho\to 0} u_\rho(\mathbf{x}) = \beta u(0)\Phi(\mathbf{x}) \quad [18]$$

where $\Phi(\mathbf{y}) = \Phi(r)$ is the radial solution of the equation **16**, $\beta = \frac{1}{\Phi(1)}$ and $u(0)$ is the value of the solution of **[17]** at the origin.

One can replace the ball B_L with an arbitrary domain $\Omega \subset \mathbb{R}^3$ containing B_L, and show that adding the bulk modulus **[6]** inside the cloaked region improves the cloaking effect (see *SI Text*)

Via homogenization, the waves in such a Schrödinger hat with anisotropic $\mathbb{M}_\rho$ are well-approximated by waves governed by the Helmholtz equation with isotropic mass densities $m_{\rho,\varepsilon}$ as $\varepsilon \to 0$. One can then use the classical Liouville gauge transformation to obtain potentials $V_{\rho,\varepsilon}$ such that, at energy $E = \omega^2$, the solutions of the Schrödinger equations $(-\nabla^2 + V_{\rho,\varepsilon} + Q_\rho)\psi = E\psi$, admit solutions with similar behavior. See the theorems below and (*SI Text*).

Scattering by a Schrödinger Hat. Now consider the effect of Schrödinger hats on scattering experiments in $\mathbb{R}^3$. In free space, a wave function Ψ satisfies

$$(-\nabla^2 - E)\Psi = 0, \quad \text{in } \mathbb{R}^3, \qquad [19]$$

and we choose $\Psi(\mathbf{x}) = \Psi^{\text{in}}(\mathbf{x}) := e^{i\omega\mathbf{e}\cdot\mathbf{x}}$, $|\mathbf{e}| = 1$, $\omega^2 = E$, a plane wave in the direction $\mathbf{e}$. We compare these with the wave functions in $\mathbb{R}^3$ scattered by the SH potential,

$$(-\nabla^2 + V_{\rho,\varepsilon} + Q_\rho - E)\Psi_{\rho,\varepsilon} = 0, \quad \text{in } \mathbb{R}^3, \qquad \Psi_{\rho,\varepsilon} = \Psi^{\text{in}} + \Psi^{\text{sc}}_{\rho,\varepsilon}, \qquad [20]$$

where $\Psi^{\text{sc}}_{\rho,\varepsilon}$ satisfies the Sommerfeld radiation condition. (Note that the SH potential is of compact support, since it vanishes outside B_2).

Since scattering data for these problems is equivalent to Dirichlet-to-Neumann operators on ∂B_L (35), one can use the results above to analyze scattering by a SH potential. We see, using [**S16**], [**S21**], and [**S24**] from (*SI Text*), that when ρ and ε are small enough the solution $\Psi_{\rho,\varepsilon}$ is close to Ψ^{in} outside B_2, close to $m_{\rho,\varepsilon}^{-1/2}(\mathbf{x})\Psi^{\text{in}}(F^{-1}(\mathbf{x}))$ in $B_2 - B_R$, and close to $\Psi^{\text{in}}(0)\Phi(\mathbf{x})$ in the cloaked region. Thus, we see that scattering observations, i.e., observables depending on the far field patterns of the solutions, are almost the same for the Schrödinger hat (when ρ and ε are small) as for empty space.

Theorems. The effects of Schrödinger hats on incident time harmonic waves are encapsulated in the following statements. Assume that $E = \omega^2$ is not a Dirichlet eigenvalue in B_L and $h \in H^{\frac{1}{2}}(S_L)$. Let w be the unique solution of $(\nabla^2 + \omega^2)w = 0$, $w|_{S_L} = h$. We assume that the radially symmetric, isotropic mass density $m_{\rho,\varepsilon}$ can be written as $m_{\rho,\varepsilon}(\mathbf{x}) = \mathbf{m}(|\mathbf{x}|, \frac{1}{\varepsilon}|\mathbf{x}|)$ where $\mathbf{m}$ is periodic function in the second variable with period 1. Below, ν and θ are the limits of $m_{\rho,\varepsilon}(\mathbf{x})^{-1/2}$ and $m_{\rho,\varepsilon}(\mathbf{x})^{-1}$, resp., in the sense of distributions, as $\varepsilon \to 0$, $\rho \to 0$. This means that $\theta(\mathbf{x})$ is the average of $r' \mapsto \mathbf{m}(|\mathbf{x}|, r')$ and $\nu(\mathbf{x})$ is the average of $r' \mapsto \sqrt{\mathbf{m}(|\mathbf{x}|, r')}$ over the interval $0 \le r' \le 1$. Below, Φ is the L^2-normalized eigenfunction satisfying [**16**].

Theorem 1. *For any R_0, R_1 and τ_2 there are parameters $\tau_1(n)$, $n \in Z_+$ and sequences $\rho_n, \rho_n', \varepsilon_n \to 0$ as $n \to \infty$, such that the solutions u_n of the acoustic equation 7 corresponding to coefficients m_{ρ_n,ε_n} and $\lambda_{\rho_n'}$ converge weakly in $L^2(B_L)$, with*

$$\tilde{u} := \lim_{n\to\infty} u_n = \begin{cases} w(\mathbf{x}), & \text{in } B_L - \overline{B}_2, \\ w(F^{-1}(\mathbf{x})), & \text{in } B_2 - \overline{B}_1, \\ w(0)\Phi(\mathbf{x}), & \text{in } B_1. \end{cases}$$

Let V_n^{sh} be the SH potential corresponding to coefficients m_{ρ_n,ε_n} and $\lambda_{\rho_n'}$ and energy E.

Theorem 2. *The solutions ψ_n of the Schrödinger equation in B_L with the SH potentials V_n^{sh}, the energy E and the Dirichlet boundary value $\psi_n|_{S_L} = h$ satisfy*

$$\lim_{n\to\infty} \psi_n = \begin{cases} w(\mathbf{x}), & \text{in } B_L - \overline{B}_2, \\ \nu(\mathbf{x})w(F^{-1}(\mathbf{x})), & \text{in } B_2 - \overline{B}_1, \\ w(0)\Phi(\mathbf{x}), & \text{in } B_1, \end{cases}$$

$$\lim_{n\to\infty} |\psi_n|^2 = \begin{cases} |w(\mathbf{x})|^2, & \text{in } B_L - \overline{B}_2, \\ \theta(\mathbf{x})|w(F^{-1}(\mathbf{x}))|^2, & \text{in } B_2 - \overline{B}_1, \\ |w(0)\Phi(\mathbf{x})|^2, & \text{in } B_1, \end{cases}$$

weakly in $L^2(B_L)$ and in the sense of distributions, resp.,

We note that $\theta(\mathbf{x})$ above is not equal to $\eta(\mathbf{x})^2$. Due to these theorems, it is natural to define $\psi^{\text{sh}}_{\text{eff}}(\mathbf{x}) := \theta(\mathbf{x})^{1/2}\tilde{u}(\mathbf{x})$, whose absolute value squared equals $\lim_{n\to\infty}|\psi_n(\mathbf{x})|^2$.

Implementations. We briefly describe possible physical realizations of Schrödinger hats for a variety of wave phenomena, first for acoustics and EM using materials with negative bulk modulus or permittivity, and then for QM via highly oscillatory potentials. (The lossy nature of presently available metamaterials will make effective implementations of Schrödinger hats technically challenging.) Details will appear elsewhere.

i. Equation **S23** with isotropic mass $m_{\rho,\varepsilon}$ and bulk modulus λ_ρ in (*SI Text*) describes an approximate acoustic cloak. The negative values of τ_2 required for the potential Q_ρ correspond to a material with negative bulk modulus; such materials have already been proposed (36). There are many designs and realizations for acoustic cloaks (6–8, 17, 37); acoustic Schrödinger hats could be implemented by placing layered negative bulk modulus material inside such a cloak. Possible implementations of acoustic cloaks, as well as potential difficulties, are discussed in (*SI Text*). Similarly, for electromagnetic waves, one can consider a cylindrical EM cloak (5) and insert in it material with negative permittivity to implement a structure similar to the SH potential. The analysis related to such cylindrical cloaks with parameters suitably chosen to create a SH potential for incident time harmonic TM-polarized waves is similar to the arguments here for the 3D spherical cloak, although with different asymptotics for [**S9**].
ii. Invisible plasmons. Surface plasmons are localized electromagnetic waves that can exist at the boundaries between materials with positive and negative electric permittivity such as dielectrics and metals (38). The localized wave inside the SH resembles a surface plasmon; however, in contrast to ordinary surface plasmons, it is hidden. These cloaked plasmons could be produced using techniques to those in 2D plasmonic cloaking (39), where the electromagnetic wave of the plasmon propagates on a glass surface covered by a gold layer with concentric rings of polymer on top. The widths and the radii of the rings can be chosen so that the structure implements an invisibility cloak for a wave localized on the surface plane. In 2D plasmonic cloaking (39), such a structure has been used to implement a nonmagnetic optical cloak (40), an approximate cloak for which the light rays are transformed according to the transformation [**3**]. Including two additional metal-dielectric rings in the interior of the cloaking structure, we can then implement a SH potential (see *SI Text* and Fig. S4). In this case the plasmon is not only confined to the surface but becomes strongly localized in the SH, while remaining invisible.
iii. Hidden matter waves. It is also possible that a SH can be produced for matter wave cloaks (9). Here one can exploit the fact that the normal roles of light and matter can be reversed: light acts like a refractive index for matter waves, see e.g., (41). Light fields can thus be used to generate the effective index distributions required for the implementation of a SH, see (42). For cold atoms confined in 2D by a light sheet, one could

APPLIED MATHEMATICS

produce the SH potentials by illuminating the sample orthogonally to the light sheet with a light beam, generated by a hologram, that carries the intensity distribution required for the SH. The result would be a highly localized matter wave that nevertheless remains hidden.

iv. Another possible path towards a solid state realization of a quantum Schrödinger hat utilizes a sufficiently large heterostructure of semiconducting materials. By homogenization theory, the SH potential can be approximated using layered potential well shells of depth $-V_-$ and barrier shells of height V_+. By rescaling the $\mathbf{x}$ coordinate we can make the values $V_\pm$ smaller; in such scaling the size of the support of the SH potential grows and E becomes smaller. This layered family of concentric potential wells and barriers can be implemented with a heterostructure of semiconducting materials. In such a structure the wave functions of electrons with energy close to the bottom of the conduction bands can be approximated using Bastard's envelope function method (43). Choosing the materials and thickness of the spherical layers suitably, the envelope functions satisfy a Schrödinger equation whose solutions are close to those for a SH potential.

ACKNOWLEDGMENTS. AG is supported by US NSF; YK by UK EPSRC; ML by Academy of Finland; UL by EPSRC and the Royal Society; and GU by US NSF, a Walker Family Endowed Professorship at UW, a Chancellor Professorship at UC, Berkeley, and a Clay Senior Award.

1. Greenleaf A, Lassas M, Uhlmann G (2003) Anisotropic conductivities that cannot be detected by EIT. *Physiol Meas* 24:413–420.
2. Greenleaf A, Lassas M, Uhlmann G (2003) On nonuniqueness for Calderon's inverse problem. *Math Res Lett* 10:685–693.
3. Leonhardt U (2006) Optical conformal mapping. *Science* 312:1777–1780.
4. Pendry J, Schurig D, Smith D (2006) Controlling electromagnetic fields. *Science* 312:1780–1782.
5. Schurig D, et al. (2006) Metamaterial electromagnetic cloak at microwave frequencies. *Science* 314:977–980.
6. Cummer S, Schurig D (2007) One path to acoustic cloaking. *New J Phys* 9:45.
7. Chen HY, Chan CT (2007) Acoustic cloaking in three dimensions using acoustic metamaterials. *Appl Phys Lett* 91:183518.
8. Cummer S, et al. (2008) Scattering theory derivation of a 3D acoustic cloaking shell. *Phys Rev Lett* 100:024301.
9. Zhang S, Genov D, Sun C, Zhang X (2008) Cloaking of matter waves. *Phys Rev Lett* 100:123002.
10. Leonhardt U, Philbin T (2006) General relativity in electrical engineering. *New J Phys* 8:247.
11. Leonhardt U, Philbin T (2009) Transformation optics and the geometry of light. *Prog Opt* 53:69–152.
12. Leonhardt U, Tyc T (2008) Broadband invisibility by non–Euclidean cloaking. *Science* 323:110–112.
13. Chen HY, Chan CT (2007) Transformation media that rotate electromagnetic fields. *Appl Phys Lett* 90:241105.
14. Greenleaf A, Kurylev Y, Lassas M, Uhlmann G (2007) Electromagnetic wormholes and virtual magnetic monopoles from metamaterials. *Phys Rev Lett* 99:183901.
15. Lai Y, et al. (2009) Illusion optics: the optical transformation of an object into another object. *Phys Rev Lett* 102:253902.
16. Leonhardt U, Philbin T (2010) *Geometry and Light: The Science of Inivisibility* (Dover, New York).
17. Greenleaf A, Kurylev Y, Lassas M, Uhlmann G (2007) Full-wave invisibility of active devices at all frequencies. *Comm Math Phys* 275:749–789.
18. Greenleaf A, Kurylev Y, Lassas M, Uhlmann G (2008) Approximate quantum cloaking and almost–trapped states. *Phys Rev Lett* 101:220404.
19. Greenleaf A, Kurylev Y, Lassas M, Uhlmann G (2011) Approximate quantum and acoustic cloaking. *J Spectral Theory* 1:27–80.
20. Kohn R, Onofrei D, Vogelius M, Weinstein M (2010) Cloaking via change of variables for the Helmholtz equation. *Comm Pure Appl Math* 63:973–1016.
21. Greenleaf A, Kurylev Y, Lassas M, Uhlmann G (2011) Cloaking a sensor via transformation optics. *Phys Rev E* 83:016603.
22. Alù A, Engheta N (2009) Cloaking a sensor. *Phys Rev Lett* 102:233901.
23. Shelby R, Smith D, Schultz S (2001) Experimental verification of a negative index of refraction. *Science* 292:77–79.
24. Li J, Chan CT (2004) Double-negative acoustic material. *Phys Rev E* 70:055602 (R).
25. Lee SH, et al. (2010) Composite acoustic medium with simultaneously negative density and modulus. *Phys Rev Lett* 104:054301.
26. Chen HY, Chan CT (2010) Acoustic cloaking and transformation acoustics. *J Phys D: Appl Phys* 43:113001.
27. Greenleaf A, Kurylev Y, Lassas M, Uhlmann G (2008) *Comment on "Scattering Theory Derivation of a 3D Acoustic Cloaking Shell"*, http://arxiv.org/abs/0801.3279.
28. Nicorovici N-A, McPhedran R, Milton G (1994) Optical and dielectric properties of partially resonant composites. *Phys Rev B* 49:8479.
29. Milton G, Nicorovici N-A, McPhedran R, Podolskiy V (2005) A proof of superlensing in the quasistatic regime, and limitations of superlenses in this regime due to anomalous localized resonance. *Proc R Soc A* 461:3999–4034.
30. Colton D, Päivärinta L, Sylvester J (2007) The interior transmission problem. *Inv Prob Imag* 1:13–28.
31. Alù A, Engheta N (2010) Cloaked near-field scanning optical microscope tip for noninvasive near-field imaging. *Phys Rev Lett* 105:263906.
32. Ruan Z, Yan M, Neff C, Qiu M (2007) Ideal cylindrical cloak: perfect but sensitive to tiny perturbations. *Phys Rev Lett* 99:113903.
33. Greenleaf A, Kurylev Y, Lassas M, Uhlmann G (2008) Isotropic transformation optics: approximate acoustic and quantum cloaking. *New J Phys* 10:115024.
34. Kohn R, Shen H, Vogelius M, Weinstein M (2008) Cloaking via change of variables in electric impedance tomography. *Inv Prob* 24:015016.
35. Berezanskii Y (1958) The uniqueness theorem in the inverse problem of spectral analysis for the Schrödinger equation (Russian). *Trudy Mosk Mat Obs* 7:1–62.
36. Wang Y, Lakes R (2005) Composites with inclusions of negative bulk modulus: extreme damping and negative Poissons ratio. *J Comp Mat* 39:1645–1657.
37. Zhang S, Xia C, Fang N (2011) Broadband acoustic cloak for ultrasound waves. *Phys Rev Lett* 106:024301.
38. Maier S (2007) *Plasmonics: Fundamentals and Applications* (Springer, Berlin).
39. Smolyaninov I, Hung Y, Davies C (2008) Two-dimensional metamaterial structure exhibiting reduced visibility at 500 nm. *Opt Lett* 33:1342–1344.
40. Cai W, Chettiar UK, Kildishev AV, Shalaev VM, Milton GW (2007) Nonmagnetic cloak with minimized scattering. *Appl Phys Lett* 91:111105.
41. Leonhardt U (2000) Space-time geometry of quantum dielectrics. *Phys Rev A* 62:012111.
42. Ashkin A (1997) Optical trapping and manipulation of neutral particles using lasers. *Proc Natl Acad Sci USA* 94:4853–4860.
43. Bastard G (1988) *Wave Mechanics Applied to Semiconductor Heterostructures* (Halsted Press, Canberra, Australia).